

Instability of a Thin Conducting Foil Accelerated by a Finite Wavelength Intense Laser

B. Eliasson¹

¹*SUPA, Physics Department, John Anderson Building,
Strathclyde University, Glasgow G4 0NG, Scotland, UK.**

(Dated: 23 July 2014)

We derive a theoretical model for the Rayleigh-Taylor (RT)-like instability for a thin foil accelerated by an intense laser, taking into account finite wavelength effects in the laser wave field. The latter leads to the diffraction of the electromagnetic wave off the periodic structures arising from the instability of the foil, which significantly modifies the growth rate of the RT-like instability when the perturbations on the foil have wavenumbers comparable to or larger than the laser wavenumber. In particular, the growth rate has a local maximum at a perturbation wavenumber approximately equal to the laser wavenumber. The standard RT instability, arising from a pressure difference between the two sides of a foil, is approximately recovered for perturbation wavenumbers smaller than the laser wavenumber. Differences in the results for circular and linear polarization of the laser light are pointed out. The model has significance to radiation pressure acceleration of thin foils and to laser-driven inertial confinement fusion schemes, where RT-like instabilities are significant obstacles.

The Rayleigh-Taylor (RT) instability, or RT-like instabilities [1], is one of the main obstacles preventing a greater success of the radiation pressure acceleration scheme for accelerating thin foils of ions by intense lasers [2–8], and in the realization of inertial confinement fusion via laser compression and heating of fuel pellets [9]. While the RT instability was originally associated with a heavier fluid on top of a lighter fluid in a gravitational field [10], similar instabilities occur for plasmas confined by magnetic fields (e.g. Ref. [14]), and when a thin foil is accelerated by the pressure difference between the two sides of the foil [1, 2]. The growth rate of the RT instability for laser accelerated plasma is typically proportional to \sqrt{gk} , where g is the acceleration and k the wavenumber of the surface perturbation. This predicts that the instability grows indefinitely for large wavenumbers; while in some experiment and simulations, the RT instability gives rise to structures with a spatial periodicity comparable to the laser wavelength [7]. The assumption of a constant normal pressure force is reasonable as long as the perturbations of the foil are relatively small and when the length-scales of the perturbations are much larger than the wavelength of the laser [2]. However, the laser light has a finite wavelength, and is scattered off the periodic structures leading to a diffraction of the electromagnetic (EM) wave. Therefore the directions of the scattered light will be quantized, and the "pressure" picture can only be expected to be approximate for monochromatic laser light. Theoretical investigations of the instabilities resulting from the scattering of EM waves off plasma surface perturbations include the RT instability of an over-dense plasma layer [11] using a magnetohydrodynamic-like model for the plasma, and the scattering off surface plasma waves [12] where the electron dynamics is the dominant source of the insta-

bility. The aim of this Letter is to solve the scattering problem and to derive a model for the instability of an ultra-thin, perfectly conducting foil accelerated by the radiation pressure of a finite wavelength intense laser.

We assume that the laser interacts with a foil where the electron density is much higher than the critical density so that no laser light penetrates the foil. We carry out the calculations in a frame moving with the velocity of the unperturbed foil. In this frame, the dynamics of the initially small-amplitude perturbations of the foil is non-relativistic. The results obtained in the moving frame can later be Lorentz transformed to the laboratory frame, but we will here for simplicity assume that the speed of the foil is non-relativistic. The velocity \mathbf{v} of the foil relative to the accelerated frame is governed by the momentum equation

$$M \left(\frac{\partial}{\partial t} + v_x \frac{\partial}{\partial x} + v_y \frac{\partial}{\partial y} \right) \mathbf{v} = \mathbf{F} - M g_0 \hat{\mathbf{z}}, \quad (1)$$

where $M(x, y, t)$ is the surface mass density, $g_0 = F_0/M_0$ is the acceleration of the unperturbed foil in the z -direction, M_0 is the unperturbed areal mass density of the foil, $F_0 = 2I_0/c$ is the radiation pressure force, I_0 is the incident laser intensity, and c the speed of light in vacuum. The force \mathbf{F} is due to the space- and time-dependent EM field acting on the foil. For an unperturbed foil, with $M = M_0$, the force \mathbf{F} would be exactly canceled by the inertial force $-M_0 g_0 \hat{\mathbf{z}}$, but due to perturbations in the foil, the forces are not exactly canceled, which will lead to the RT-like instability. The mass density is governed by the continuity equation

$$\frac{\partial M}{\partial t} + \frac{\partial(Mv_x)}{\partial x} + \frac{\partial(Mv_y)}{\partial y} = 0. \quad (2)$$

The foil surface can be parameterized as $S(x, y, z, t) = z - \eta(x, y, t) = 0$, where η is the surface elevation of the foil in the z -direction. The velocity and surface elevation

*Electronic address: bengt.eliasson@strath.ac.uk

are connected through the kinematic condition

$$\frac{\partial \eta}{\partial t} = \mathbf{v} \cdot \nabla S. \quad (3)$$

Equations (1)–(3) are completed by initial conditions on η and on M and \mathbf{v} at $z = \eta$.

First we notice that the assumption of a constant radiation pressure force F_0 acting perpendicularly to the surface on one side of the foil [1, 2] would lead to that $\mathbf{F} = F_0 \nabla S$ in Eq. (1) and to a “standard” RT instability with the growth rate $\sqrt{g_0 k}$. Here we will instead determine \mathbf{F} by taking into account that the electric and magnetic fields \mathbf{E} and \mathbf{B} evolve in time according to Maxwell’s equations, obeying boundary conditions at the foil surface as well as radiating boundary conditions far away from the foil. We assume that the foil is perfectly conducting, and therefore the electric field parallel to the surface and the magnetic field perpendicular to the surface are zero in a system (denoted by primed variables) moving with the same velocity as the surface, with the boundary conditions expressed as $\mathbf{E}' \times \nabla S = 0$ and $\mathbf{B}' \cdot \nabla S = 0$ at $z = \eta$. Assuming non-relativistic velocities in the moving frame, the magnetic and electric fields are Galilei transformed from the system moving with the foil surface (primed variables) to the accelerated frame (unprimed variables) as $\mathbf{E}' = \mathbf{E} + \mathbf{v} \times \mathbf{B}$ and $\mathbf{B}' = \mathbf{B} - \mathbf{v} \times \mathbf{E}/c^2 \approx \mathbf{B}$. (The term $-\mathbf{v} \times \mathbf{E}/c^2$ will only contribute to the boundary conditions with terms of order v^2/c^2 compared to unity, and is therefore neglected.) This gives

$$\mathbf{B} \cdot \nabla S = 0 \quad (4)$$

for the magnetic field, while for the electric field we have $0 = \mathbf{E}' \times \nabla S = (\mathbf{E} + \mathbf{v} \times \mathbf{B}) \times \nabla S = \mathbf{E} \times \nabla S - \mathbf{v}(\mathbf{B} \cdot \nabla S) + \mathbf{B}(\mathbf{v} \cdot \nabla S)$, where $\mathbf{B} \cdot \nabla S = 0$ and $\mathbf{v} \cdot \nabla S = \partial \eta / \partial t$, giving

$$\mathbf{E} \times \nabla S + \mathbf{B} \frac{\partial \eta}{\partial t} = 0 \quad (5)$$

at $z = \eta$.

The force acting on the surface can be calculated using the EM volume force [13]

$$\mathbf{f} = \nabla \cdot \bar{\boldsymbol{\sigma}} - \epsilon_0 \frac{\partial}{\partial t} \mathbf{E} \times \mathbf{B}, \quad (6)$$

where

$$\sigma_{ij} = \epsilon_0 \left(E_i E_j - \frac{1}{2} \delta_{ij} E^2 \right) + \frac{1}{\mu_0} \left(B_i B_j - \frac{1}{2} \delta_{ij} B^2 \right) \quad (7)$$

is the Maxwell stress tensor on component form, δ_{ij} represents the unit tensor, ϵ_0 is the electric permittivity in vacuum, and $\mu_0 = 1/(\epsilon_0 c^2)$ is the magnetic permeability in vacuum. Integrating \mathbf{f} from $z = \eta - \varepsilon$ to $\eta + \varepsilon$, assuming that \mathbf{E} and \mathbf{B} are zero for $z > \eta$, and letting $\varepsilon \rightarrow 0$ gives the EM area force $\mathbf{F} = -\bar{\boldsymbol{\sigma}} \cdot \nabla S - \epsilon_0 \mathbf{E} \times \mathbf{B} \partial \eta / \partial t$, which, using the boundary conditions (4) and (5), simplifies to

$$\mathbf{F} = \frac{1}{2} \left(\frac{B^2}{\mu_0} - \epsilon_0 E^2 \right) \nabla S. \quad (8)$$

It should be emphasized that in Eq. (8), \mathbf{E} and \mathbf{B} are the total electric and magnetic fields at the foil surface, to be determined below.

Perturbing and linearizing the system of equations (1)–(3) and (8) around the equilibrium solution $\mathbf{v} = 0$, $\eta = 0$, $M = M_0$, $S = z$, $\mathbf{E} = \mathbf{E}_0(t)$, and $\mathbf{B} = \mathbf{B}_0(t)$, gives

$$\frac{\partial^4 \eta_1}{\partial t^4} + \frac{F_0^2}{M_0^2} \left(\frac{\partial^2 \eta_1}{\partial x^2} + \frac{\partial^2 \eta_1}{\partial y^2} \right) = \frac{1}{M_0} \frac{\partial^2}{\partial t^2} \left(\frac{\mathbf{B}_0 \cdot \mathbf{B}_1}{\mu_0} - \epsilon_0 \mathbf{E}_0 \cdot \mathbf{E}_1 \right), \quad (9)$$

where the subscript 1 denotes small-amplitude, first-order perturbations. For circularly polarized light, the zeroth order EM force is

$$F_0 = \frac{1}{2} \left(\frac{B_0^2}{\mu_0} - \epsilon_0 E_0^2 \right), \quad (10)$$

while for linearly polarized light a time averaging over one laser period removes second harmonics and reduces F_0 a factor 2 for given amplitudes B_0 and E_0 . Equation (9) is completed by finding the dependence of \mathbf{E}_1 and \mathbf{B}_1 on η_1 . The general form of Eq. (9) is that of a mode-coupling equation, where the low-frequency perturbations of the foil are driven by the coupling (beating) between the large amplitude EM wave (\mathbf{B}_0 , \mathbf{E}_0) and its small-amplitude side-bands (\mathbf{B}_1 , \mathbf{E}_1).

Writing out the components of the boundary conditions (4) and (5) gives

$$B_z - B_x \frac{\partial \eta}{\partial x} - B_y \frac{\partial \eta}{\partial y} = 0, \quad (11)$$

$$E_y + E_z \frac{\partial \eta}{\partial y} + B_x \frac{\partial \eta}{\partial t} = 0, \quad (12)$$

and

$$E_x + E_z \frac{\partial \eta}{\partial x} - B_y \frac{\partial \eta}{\partial t} = 0, \quad (13)$$

at $z = \eta$. An incident EM wave will be reflected by the foil, and perturbations in the foil surface will lead to the refraction of the wave. The electric and magnetic fields can be written $\mathbf{E} = \mathbf{E}_{i0} + \mathbf{E}_r$ and $\mathbf{B} = \mathbf{B}_{i0} + \mathbf{B}_r$, where \mathbf{E}_{i0} and \mathbf{B}_{i0} are the fields of the incident wave and \mathbf{E}_r and \mathbf{B}_r of the reflected wave. In what follows, we will show details of the calculations for a circularly polarized incident wave, and at the end only state the final result also for a linearly polarized wave. More details of the derivations will be given elsewhere. For an incident, right-hand circularly polarized EM wave propagating in the z -direction, we have

$$\mathbf{E}_{i0} = \frac{\hat{\mathbf{e}}}{2} \hat{E}_{i0} e^{i\theta_i} + \text{c.c.} \quad (14)$$

and

$$\mathbf{B}_{i0} = \frac{\hat{\mathbf{e}}}{2} \hat{B}_{i0} e^{i\theta_i} + \text{c.c.}, \quad (15)$$

where $\hat{\mathbf{e}} = \hat{\mathbf{x}} + i\hat{\mathbf{y}}$ describes the polarization, $\hat{\mathbf{x}}$ and $\hat{\mathbf{y}}$ are unit vectors in the x - and y -direction, $\theta_i = k_0 z - \omega_0 t$ is the phase of the incident wave, k_0 is the incident wave-number, $\omega_0 = ck_0$ the frequency, and $\hat{E}_{i0} = ic\hat{B}_{i0}$. For linearly polarized light with the electric field along the x -axis, we would instead have $\mathbf{E}_{i0} = (\hat{\mathbf{x}}/2)\hat{E}_{i0} \exp(i\theta_i) + \text{c.c.}$, $\mathbf{B}_{i0} = (\hat{\mathbf{y}}/2)\hat{B}_{i0} \exp(i\theta_i) + \text{c.c.}$, and $\hat{E}_{i0} = c\hat{B}_{i0}$. We next assume small perturbations of the surface, so that $\eta(x, y, t) = \eta_1(x, y, t)$, where $|\nabla||\eta_1| \ll 1$. (It implies small wave steepness $|\nabla\eta_1| \ll 1$ and that $|\eta_1\nabla| \ll 1$ when acting on \mathbf{E} and \mathbf{B} .) Then $\mathbf{E}_{z=\eta} \approx \mathbf{E}_{0,z=0} + \mathbf{E}_{1,z=0} + \eta_1(\partial\mathbf{E}_0/\partial z)_{z=0}$ and $\mathbf{B}_{z=\eta} \approx \mathbf{B}_{0,z=0} + \mathbf{B}_{1,z=0} + \eta_1(\partial\mathbf{B}_0/\partial z)_{z=0}$, where $|\mathbf{E}_1| \ll |\mathbf{E}_0|$ and $|\mathbf{B}_1| \ll |\mathbf{B}_0|$. At $z = 0$, we have $\theta_i = \theta_0 = -\omega_0 t$. Writing $\mathbf{E}_r = \tilde{\mathbf{E}}_r e^{i\theta_0}/2 + \text{c.c.}$ and $\mathbf{B}_r = \tilde{\mathbf{B}}_r e^{i\theta_0}/2 + \text{c.c.}$, and linearizing the boundary conditions (11)–(13), we have at $z = 0$,

$$\tilde{B}_{rz1} - \tilde{B}_{rx0} \frac{\partial\eta_1}{\partial x} - \tilde{B}_{ry0} \frac{\partial\eta_1}{\partial y} = \hat{B}_{i0} \left(\frac{\partial\eta_1}{\partial x} + i \frac{\partial\eta_1}{\partial y} \right), \quad (16)$$

$$\tilde{E}_{ry1} + \eta_1 \frac{\partial\tilde{E}_{ry0}}{\partial z} + \tilde{B}_{rx0} \frac{\partial\eta_1}{\partial t} = \hat{B}_{i0} \left(i\omega_0\eta_1 - \frac{\partial\eta_1}{\partial t} \right), \quad (17)$$

and

$$\tilde{E}_{rx1} + \eta_1 \frac{\partial\tilde{E}_{rx0}}{\partial z} - \tilde{B}_{ry0} \frac{\partial\eta_1}{\partial t} = -i\hat{B}_{i0} \left(i\omega_0\eta_1 - \frac{\partial\eta_1}{\partial t} \right). \quad (18)$$

To zeroth order, the boundary conditions at the foil surface $z = 0$ is that the electric field parallel to the foil is zero, $\mathbf{E}_0 = 0$, and therefore $\mathbf{E}_{r0} = -\mathbf{E}_{i0}$, and it follows from Maxwell's equations that $\mathbf{B}_{r0} = +\mathbf{B}_{i0}$ at $z = 0$. Since $\mathbf{E}_0 = 0$ and $\mathbf{B}_0 = 2\mathbf{B}_{i0}$ in Eqs. (9) and (10), it is apparent that the foil is accelerated by the magnetic pressure of the EM field. The unidirectional wave equations $\partial\mathbf{E}_{r0}/\partial t - c\partial\mathbf{E}_{r0}/\partial z = 0$ and $\partial\mathbf{B}_{r0}/\partial t - c\partial\mathbf{B}_{r0}/\partial z = 0$ of the reflected wave have the boundary conditions $\mathbf{E}_{r0} = -(\hat{\mathbf{e}}/2)\hat{E}_{i0}e^{i\theta_0(t)} + \text{c.c.}$, and $\mathbf{B}_{r0} = (\hat{\mathbf{e}}/2)\hat{B}_{i0}e^{i\theta_0(t)} + \text{c.c.}$, at $z = 0$, with the solutions $\mathbf{E}_{r0} = -(\hat{\mathbf{e}}/2)\hat{E}_{i0}e^{i\theta_0(t')} + \text{c.c.}$ and $\mathbf{B}_{r0} = (\hat{\mathbf{e}}/2)\hat{B}_{i0}e^{i\theta_0(t')} + \text{c.c.}$, where the retarded time t' is obtained from $ct' = \xi$ with $\xi = z + ct$. It follows that $\tilde{\mathbf{E}}_{r0} = -\hat{\mathbf{e}}\hat{E}_{i0}e^{i\theta_0(t')-i\theta_0(t)}$ and $\tilde{\mathbf{B}}_{r0} = \hat{\mathbf{e}}\hat{B}_{i0}e^{i\theta_0(t')-i\theta_0(t)}$. Using that $\partial t'/\partial z = 1/c$ and $\hat{E}_{i0} = ic\hat{B}_{i0}$, we have $\tilde{\mathbf{E}}_{r0}|_{z=0} = -i\hat{\mathbf{e}}c\hat{B}_{i0}$, $\tilde{\mathbf{B}}_{r0}|_{z=0} = \hat{\mathbf{e}}\hat{B}_{i0}$, $\partial\tilde{\mathbf{E}}_{r0}/\partial z|_{z=0} = -\hat{\mathbf{e}}\omega_0\hat{B}_{i0}$, and $\partial\tilde{\mathbf{B}}_{r0}/\partial z|_{z=0} = -i\hat{\mathbf{e}}k_0\hat{B}_{i0}$, which is used in Eqs. (16)–(18).

We assume a 4-wave model in which the EM wave is scattered into two EM sidebands off the ripples in the foil surface, so that $\tilde{\mathbf{E}}_{r1} = \hat{\mathbf{E}}_{r1+} \exp(-i\omega t + ik_x x + ik_y y + ik_z z) + \hat{\mathbf{E}}_{r1-} \exp(i\omega^* t - ik_x x - ik_y y - ik_z^* z)$, $\tilde{\mathbf{B}}_{r1} = \hat{\mathbf{B}}_{r1+} \exp(-i\omega t + ik_x x + ik_y y + ik_z z) + \hat{\mathbf{B}}_{r1-} \exp(i\omega^* t - ik_x x - ik_y y - ik_z^* z)$, and $\eta_1 = \hat{\eta}_1 \exp(-i\omega t + ik_x x + ik_y y) + \hat{\eta}_1^* \exp(i\omega^* t - ik_x x - ik_y y)$. The vacuum wave equations for the scattered light, $\partial^2\mathbf{E}_{r1}/\partial t^2 - c^2\nabla^2\mathbf{E}_{r1} = 0$ and $\partial^2\mathbf{B}_{r1}/\partial t^2 - c^2\nabla^2\mathbf{B}_{r1} = 0$, then give the dispersion

relation

$$(\pm\omega + ck_0)^2 - c^2(k_\perp^2 + k_{z\pm}^2) = 0, \quad (19)$$

where $k_\perp^2 = k_x^2 + k_y^2$. Equation (19) has the solutions $k_{z\pm} = \mp\sqrt{(k_0 \pm \omega/c)^2 - k_\perp^2}$, where the branches of the square root are chosen such that $\text{imag}(k_{z\pm}) < 0$ for $\text{imag}(\omega) > 0$. This gives radiating boundary conditions with waves propagating out from the foil and vanishing at $z = -\infty$, which is consistent with the model. For $k_0 > k_\perp$, the scattered wave is diffracted and propagates out from the foil at an angle φ to the negative z -axis, given by $\sin\varphi \approx k_\perp/k_0$, while for $k_0 < k_\perp$ the scattered wave is evanescent and decays rapidly with the distance from the foil. Separating wave modes proportional to $\exp(-i\omega t + ik_x x + ik_y y)$ and $\exp(i\omega^* t - ik_x x - ik_y y)$, the boundary conditions (16)–(18) yield the Fourier coefficients $\hat{B}_{rz1+} = 2\hat{B}_{i0}(ik_x - k_y)\hat{\eta}_1$, $\hat{B}_{rz1-} = 2\hat{B}_{i0}^*(ik_x + k_y)\hat{\eta}_1$, $\hat{E}_{ry1+} = 2i\hat{B}_{i0}(\omega_0 + \omega)\hat{\eta}_1$, $\hat{E}_{ry1-} = -2i\hat{B}_{i0}^*(\omega_0 - \omega)\hat{\eta}_1$, $\hat{E}_{rx1+} = 2\hat{B}_{i0}(\omega_0 + \omega)\hat{\eta}_1$, and $\hat{E}_{rx1-} = 2\hat{B}_{i0}^*(\omega_0 - \omega)\hat{\eta}_1$. From the divergence condition $\nabla \cdot \mathbf{E}_r = 0$ to the left of the foil, we obtain $\hat{E}_{rz1+} = -2\hat{B}_{i0}(\omega_0 + \omega)(k_x + ik_y)\hat{\eta}_1/k_{z+}$ and $\hat{E}_{rz1-} = -2\hat{B}_{i0}^*(\omega_0 - \omega)(k_x - ik_y)\hat{\eta}_1/k_{z-}$, and from the x - and y -components of Faraday's law $\partial\mathbf{B}_r/\partial t = -\nabla \times \mathbf{E}_r$, we have $\hat{B}_{rx1+} = -2i\hat{B}_{i0}(k_y^2 + k_{z+}^2 - ik_x k_y)\hat{\eta}_1/k_{z+}$, $\hat{B}_{ry1+} = 2\hat{B}_{i0}(k_x^2 + k_{z+}^2 + ik_x k_y)\hat{\eta}_1/k_{z+}$, $\hat{B}_{rx1-} = -2i\hat{B}_{i0}^*(k_y^2 + k_{z-}^2 + ik_x k_y)\hat{\eta}_1/k_{z-}$, and $\hat{B}_{ry1-} = -2\hat{B}_{i0}^*(k_x^2 + k_{z-}^2 - ik_x k_y)\hat{\eta}_1/k_{z-}$.

We next insert these results into Eq. (9) and separate terms proportional to $\exp(-i\omega t + ik_x x + ik_y y)$ and/or $\exp(i\omega^* t - ik_x x - ik_y y)$. This gives the dispersion relation for the RT-like instability for circularly polarized incident laser light,

$$\omega^4 - g_0^2 k_\perp^2 = i \frac{\omega^2 g_0}{2} \sum_{+,-} \frac{k_\perp^2 + 2k_{z\pm}^2}{k_{z\pm}}, \quad (20)$$

where $k_{z\pm}$ is given by the solutions of Eq. (19), and $g_0 = F_0/M_0$. An analogous calculation for linearly polarized light with $\mathbf{E}_{i0} = (\hat{\mathbf{x}}/2)\hat{E}_{i0} \exp(i\theta_i) + \text{c.c.}$, $\mathbf{B}_{i0} = (\hat{\mathbf{y}}/2)\hat{B}_{i0} \exp(i\theta_i) + \text{c.c.}$, and $\hat{E}_{i0} = c\hat{B}_{i0}$ yields the dispersion relation

$$\omega^4 - g_0^2 k_\perp^2 = i\omega^2 g_0 \sum_{+,-} \frac{k_x^2 + k_{z\pm}^2}{k_{z\pm}}. \quad (21)$$

The dispersion relations (20) and (21) have one positive imaginary root $\omega = i\omega_I$, which gives rise to a purely growing instability with growth rate ω_I . If the right-hand sides of Eqs. (20) and (21) are neglected, then we recover the standard RT instability with the growth-rate $\omega_I = \sqrt{g_0 k_\perp}$. There also exist two real-valued roots which give rise to oscillatory solutions, similarly as for the standard RT instability [1]. To compare with experiments and simulations, we notice first that a critical dimensionless parameter of the system is the normalized acceleration $g_0/(c^2 k_0)$, which can be expressed

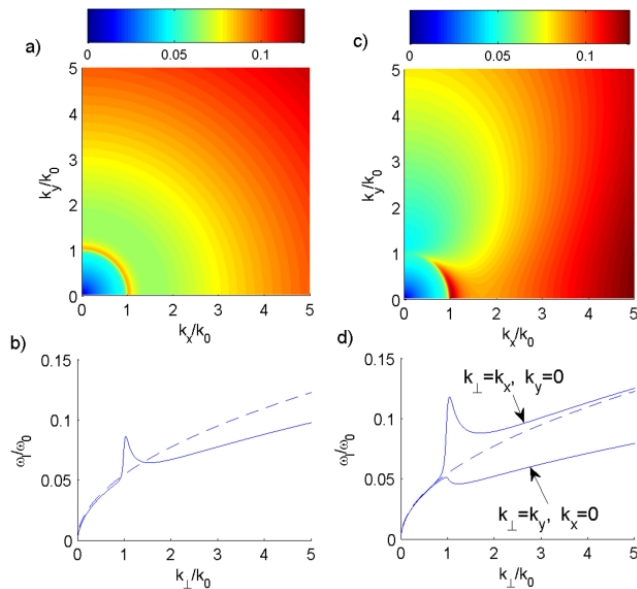


FIG. 1: The normalized growth rate ω_I/ω_0 of the instability for circularly polarized waves [panels a), b)] obtained from Eq. (20), and linearly polarized waves [panels c), d)] obtained from Eq. (21). Top panels a), c) show color plots of the growth rate as a function of $(k_x/k_0, k_y/k_0)$, while the lower panels b), d) show line plots of the growth rate (solid lines). A comparison is made with the standard Rayleigh-Taylor instability (dashed line).

in terms of commonly used laser-plasma parameters as $g_0/(c^2 k_0) = 2\sigma(Z_i m_e/m_i)(n_{cr}/n_e)a_0^2/(k_0 d)$, where Z_i is the charge state of the ions, m_e and m_i the electron and ion mass, n_e/n_{cr} is the ratio of the electron density to the critical density, $a_0 = eE_{i0}/(m_e c \omega_0)$ is the normalized laser amplitude, d is the foil thickness, and the coefficient $\sigma = 1/2$ for linearly polarized light and $\sigma = 1$ for circularly polarized light. For example, Yan et al. [3] used circularly polarized light ($\sigma = 1$) in their simulations to study the radiation pressure acceleration of a

proton H^+ foil ($Z_i = 1, m_i = 1836m_e$) with $n_0/n_{cr} = 10$, $k_0 d = 0.63$, and $a_0 = 5$, giving $g_0/(c^2 k) \approx 4.3 \times 10^{-3}$. On the other hand, Palmer et al. [7] used linearly polarized light ($\sigma = 1/2$) in their experimental and simulation study of the RT instability of a carbon C^{6+} foil ($Z_i = 6, m_i \approx 12 \times 1836 \times m_e$) with $n_e/n_{cr} = 10^3$, and $k_0 d = 0.03$. Using their values $a_0 = 10$ and $a_0 = 20$ gives $g_0/(c^2 k) \approx 9.1 \times 10^{-4}$ and 3.6×10^{-3} , respectively.

Figure 1 shows the growth rates of the instability for a typical value $g_0/(c^2 k) = 3 \times 10^{-3}$. For the case of circularly polarized light, it is noticeable from Figs. 1a and 1b that the growth rate of the instability is close to the one of the standard RT instability for $k_\perp < k_0$, has a sharply peaked maximum at $k_\perp \approx k_0$, and has a lower growth-rate than the standard RT instability for $k_\perp \gtrsim 1.5k_0$. For linearly polarized light, we see in Figs. 1c and 1d that the instability is strongly anisotropic, with a larger growth rate for perturbation wavenumbers in the x -direction, parallel to the electric field and perpendicular to the magnetic field of the incident EM wave. Similar situations often occur in plasmas confined by a non-oscillatory magnetic field and gives rise to RT-like instabilities, such as the gravitational and flute instabilities [14], where the perturbation wavenumbers of the fastest growing unstable waves are at angles almost perpendicular to the magnetic field. The RT-like instability has also a large growth rate for $k_\perp \gg k_0$, where the instability can be expected to saturate nonlinearly by forming small-scale structures but without disrupting the foil. The most severe instability is at $k_\perp \approx k_0$, which leads to the disruption of the foil and to the broadening of the energy spectrum [6]. A scheme tailored to reduce the maximum of the growth rate at $k_\perp \approx k_0$ of the RT-like instability could potentially make laser driven radiation pressure acceleration and compression schemes more tractable.

Acknowledgments Useful discussions with C. S. Liu, X. Shao and T. C. Liu at University of Maryland, and Z.-M. Cheng, T. Heelis, and A. W. Cross at University of Strathclyde are gratefully acknowledged.

-
- [1] E. Ott, Phys. Rev. Lett. **29**, 1429 (1972).
[2] F. Pegoraro and S. V. Bulanov, Phys. Rev. Lett. **99**, 065002 (2007).
[3] X. Q. Yan, C. Lin, Z. M. Sheng, Z. Y. Guo, B. C. Liu, Y. R. Lu, J. X. Fang, and J. E. Chen, Phys. Rev. Lett. **100**, 135003 (2008).
[4] M. Chen, A. Pukhov, Z. M. Sheng and X. Q. Yan, Phys. Plasmas **15**, 113103 (2008).
[5] A. P. L. Robinson, M. Zepf, S. Kar, R.G. Evans, and C. Bellei, New J. Phys. **10**, 013021 (2008).
[6] T.-C. Liu, X. Shao, C.-S. Liu, J.-J. Su, B. Eliasson, V. Tripathi, G. Dudnikova, and R. Z. Sagdeev, Phys. Plasmas **18**, 123105 (2011).
[7] C. A. J. Palmer, J. Schreiber, S. R. Nagel, N. P. Dover, C. Bellei, F. N. Beg, S. Bott, R. J. Clarke, A. E. Dangor, S. M. Hassan, P. Hilz, D. Jung, S. Kneip, S. P. D. Man-
gles, K. L. Lancaster, A. Rehman, A. P. L. Robinson, C. Spindloe, J. Szerypo, M. Tatarakis, M. Yeung, M. Zepf, and Z. Najmudin, Phys. Rev. Lett. **108**, 225002 (2012).
[8] K. Adusumilli, D. Goyal, and V. K. Tripathi, Phys. Plasmas **19**, 013102 (2012).
[9] H. Takabe, K. Mima, L. Montierth and R. L. Morse, Phys. Fluids **28**, 3676 (1985); R. Betti, V. N. Goncharov, R. L. McCrory, P. Sorotokin, and C. P. Verdon, Phys. Plasmas **3**, 2122 (1996); J. D. Kilkenny, S. G. Glendinning, S. W. Haan, B. A. Hammel, J. D. Lindl, D. Munro, B. A. Remington, S. V. Weber, J. P. Knauer, and C. P. Verdon, Phys. Plasmas **1**, 1379 (1994); J. D. Hager, T. J. B. Collins, V. A. Smalyuk, J. P. Knauer, D. D. Meyerhofer, and T. C. Sangster, Phys. Plasmas **20**, 072707 (2013).
[10] Lord Rayleigh, Proc. London Math. Soc. **14**, 170 (1882);

- G. I. Taylor, Proc. R. Soc. London Ser. A **201**, 192 (1950).
- [11] E. G. Gamaly, Phys. Rev. E **48**, 2924 (1993).
- [12] A. Macchi, F. Cornolti, and F. Pegoraro, Phys. Plasmas **9**, 1704 (2002).
- [13] J. D. Jackson, *Classical Electrodynamics*, 3rd. ed. (John Wiley & Sons, Inc., New York 1999).
- [14] R. J. Goldston and P. H. Rutherford, *Introduction to Plasma Physics* (IoP Publishing, Ltd, Philadelphia 1997).